

Synthesis, Structure, and Conductivity of the New Ternary Chalcogenide NbPdTe₅

ERIC W. LIIMATTA AND JAMES A. IBERS*

Department of Chemistry, Northwestern University, Evanston, Illinois 60208

Received April 1, 1988; in revised form June 28, 1988

The new ternary chalcogenide NbPdTe₅ has been prepared by reaction among the elements at 700/750°C. NbPdTe₅ crystallizes with four formula units in a cell with dimensions $a = 15.673(9)$ Å, $b = 3.728(2)$ Å, $c = 12.720(6)$ Å in space group D_{2h}^{16} - $Pnma$ of the orthorhombic system. The structure has been refined to a final R index on F_o^2 of 0.097 for 43 variables and 1786 observations. NbPdTe₅ displays a new layered structural type. Each layer is composed of bicapped trigonal prismatic Nb atoms and octahedral Pd atoms coordinated by Te atoms. Electrical conductivity measurements show that NbPdTe₅ is metallic; $\sigma_{295} \approx 1.3 \times 10^3 \Omega^{-1} \text{ cm}^{-1}$. Although structurally NbPdTe₅ is very similar to NbNiTe₅, their electrical conductivity behavior is vastly different. © 1988 Academic Press, Inc.

Introduction

Instead of describing solid-state structures as cations filling vacancies in a closest packed anion array, one may describe many solid-state structures as metal-centered polyhedra that are linked together to form larger assemblies. Thus, one may try to synthesize new materials by substituting one metal for another one with similar coordination preferences. We have made such attempts in an area of chemistry we are actively studying, the Group V ternary tellurides (1, 2). This interest in the tellurides stems from the fact that the binary Group V tellurides possess some interesting structural (3, 4) and physical (5-7) properties. Also this chemistry is intriguing because the ternary tellurides in this system crystallize in structural types different from those

found in the sulfides and selenides (1, 2). Our initial efforts led to the synthesis of NbNiTe₅ (1). Pd and Ni have similar coordination preferences in the tellurides (8-10) and we have been able to substitute Pd for Ni to prepare the new compound NbPdTe₅. Here we report its synthesis, structure, and conductivity.

Experimental

Synthesis. The compound NbPdTe₅ was synthesized from powders of the elements (Nb, 99.8%, Aesar; Pd, 99.95%, Alfa; Te, 99.99%, Aesar). These were loaded in a silica tube in the atomic ratio Nb: Pd: Te = 3: 1: 8. This ratio of the elements was used because it has been successful in the preparation of other new tellurides (1, 2). A large amount of I₂ ($\approx 15\%$ by wt) was added as a transport agent and appears to be necessary for crystal growth. The tube was evacuated

* To whom all correspondence should be addressed.

to $\approx 10^{-5}$ Torr and then sealed. The tube was then heated under a temperature gradient of 700/750°C for 8 days. A small amount of very thin needle-like crystals formed. Analysis of these crystals with the microprobe of an EDAX equipped Hitachi S570 scanning electron microscope showed the presence of Nb, Pd, and Te, but not of I. Quantitative analysis on four crystals was performed with use of the program MICROQ (11). Crystals of $Ta_3Pd_3Te_{14}$ and $NbNiTe_5$ were the standards used in this procedure. The analysis gave Nb, 10.87(24); Pd, 14.16(47); Te, 74.96(61). Calculated for $NbPdTe_5$: Nb, 11.09; Pd, 12.71; Te, 76.19. Although these analytical results are slightly outside the claimed accuracy of ± 1 wt% for the program MICROQ, these results still confirm the composition of the crystals.

Conductivity. A single crystal of $NbPdTe_5$ of average dimensions $0.013 \times 0.013 \times 1$ mm was mounted with Ag paint on the Al wires of an integrated circuit chip. The chip was placed in a sample holder within a metal Dewar in a reservoir of liquid He. The temperature was regulated by controlling the rate of blow off of He gas. Four-probe ac conductivity measurements along the needle axis b were then performed with equipment and procedures described previously (12).

Structure determination. Weissenberg photographs established the orthorhombic symmetry and approximate cell parameters of $NbPdTe_5$. The final cell parameters were determined from least-squares analysis of the setting angles of 18 reflections in the range of $21^\circ \leq 2\theta$ ($MoK\alpha_1$) $< 32^\circ$ automatically centered on an Enraf-Nonius CAD4 diffractometer. Diffraction data were collected at $-150^\circ C$. Six standard reflections, measured every 3 hr, showed no significant variation in intensity. Table I gives details of the data collection.

All calculations were carried out on a Harris 1000 computer with programs and

TABLE I
CRYSTAL DATA FOR $NbPdTe_5$

Formula mass (amu)	837.31
Space group	$D_{2h}^{16}-Pnma$
a (Å)	15.673(9) ^a
b (Å)	3.728(2)
c (Å)	12.720(6)
V (Å ³)	743.2
Z	4
T of data collection (K) ^b	123
Density (calc) (g cm ⁻³)	7.48
Radiation (graphite monochromated)	$MoK\alpha_1$ ($\lambda(K\alpha_1) = 0.7093$ Å)
Crystal shape	Flattened rod bounded by {010} {100} {001}
Crystal vol. (mm ³)	2.46×10^{-5}
Linear abs. coeff. (cm ⁻¹)	230.5
Transmission factors ^c	0.22–0.85
Detector aperture (mm)	Horizontal 4.0, vertical 2.5
Takeoff angle (deg)	3.5
Scan type	θ - 2θ
Scan speed (deg min ⁻¹)	1.37 ^c
Scan range (deg)	1.0 below $K\alpha_1$ to 1.0 above $K\alpha_2$
Background counts	1/4 of scan range on each side of reflection
θ limits (deg)	$3 < \theta < 35.0$
Data collected	$h, \pm k, l$
p factor	0.04
No. of data collected	3366
No. of unique data	1786
No. of unique data with $F_o^2 > 3\sigma(F_o^2)$	890
$R(F^2)$	0.097
$R_w(F^2)$	0.123
R (on F for $F_o^2 > 3\sigma(F_o^2)$)	0.043
Error in obs. of unit weight (e^2)	0.90

^a Obtained from a refinement constrained so that $\alpha = \beta = \gamma = 90^\circ$.

^b The low-temperature system for the Nonius CAD4 diffractometer is from a design by Professor J. J. Bonnet and S. Askenazy and is commercially available from Sotorem, Castanet-Tolosan, France.

^c Reflections with $\sigma(I)/I > 0.33$ were rescanned up to a maximum time of 100 sec.

methods standard in this laboratory (13). Conventional atomic scattering factors (14) were used and anomalous dispersion corrections (15) were applied. The processed data were corrected for absorption. The systematic extinctions ($0kl, k + l = 2n + 1$; $hk0, h = 2n + 1$) are consistent with the space groups $Pnma$ and $Pn2_1a$. The former was chosen since a satisfactory residual of 0.071 resulted from averaging the absorption corrected inner sphere ($2\theta < 50^\circ$) data with $F_o^2 > 3\sigma(F_o^2)$ in mmm symmetry. All of the atomic positions were found with the use of the program SHELXS-86 (16). The

TABLE II
POSITIONAL AND EQUIVALENT ISOTROPIC THERMAL
PARAMETERS FOR NbPdTe₅

Atom	Wyckoff notation	x	y	z	B _{eq} (Å ²)
Te(1)	4c	0.179318(76)	1/4	0.13230(10)	0.46(2)
Te(2)	4c	0.235846(74)	3/4	0.35541(10)	0.39(2)
Te(3)	4c	-0.057597(75)	3/4	0.131355(98)	0.39(2)
Te(4)	4c	0.008332(74)	1/4	0.34811(10)	0.40(2)
Te(5)	4c	0.348228(79)	3/4	0.080943(97)	0.44(2)
Pd	4c	0.091600(89)	3/4	0.23878(12)	0.42(3)
Nb	4c	0.34193(10)	1/4	0.24856(13)	0.29(3)

structure was refined by least-squares methods. The function minimized was $\Sigma w(F_o^2 - F_c^2)^2$. The final cycle of refinement on F_o^2 included anisotropic thermal parameters and resulted in a value of $R(F_o^2)$ of 0.097. The value for the conventional R (on F for $F_o^2 > 3\sigma(F_c^2)$) is 0.043. The final difference electron density map shows no peak higher than 3.5% the height of a Te atom. No unusual trends were found in an analysis of F_o^2 vs F_c^2 as a function of F_o^2 , setting angles, and Miller indices. The refined values of the thermal parameters and the analytical data are both consistent with a stoichiometric structure. The satisfactory refinement justifies the choice of the centrosymmetric space group $Pnma$. Final values of the positional parameters appear in Table II. Final anisotropic thermal parameters and structure amplitudes are given in Tables III¹ and IV¹.

Results

Interatomic distances and angles for NbPdTe₅ are given in Table V. A view down the b axis (Fig. 1a) clearly shows the

¹ See NAPS Document No. 04619 for 9 pages of supplementary materials from ASIS/NAPS, Microfiche Publications, P.O. Box 3513, Grand Central Station, New York, NY 10163. Remit in advance \$4.00 for microfiche copy or for photocopy, \$7.75. All orders must be prepaid.

layered nature of the structure. In this structure there are two unique chains that run parallel to the b axis. The chains consist of face-sharing Nb-centered bicapped trigonal prisms and edge-sharing Pd-centered octahedra. Figure 2a clearly displays the geometry around the Nb and Pd atoms. NbPdTe₅ forms in a new structural type that is very similar to that of NbNiTe₅. NbNiTe₅ is also a layered material that possesses two unique chains. One chain consists of Nb-centered bicapped trigonal prisms that share triangular faces and the other chain is made up of Ni-centered edge-sharing octahedra. Figures 1b and 2b show two drawings of the NbNiTe₅ structure. These drawings can be compared with Figs. 1a and 2a which depict the NbPdTe₅ structure. From this comparison, and from the description of the coordination environments around the metal atoms in these structures, it is apparent that there is a strong correspondence between structures

TABLE V
SELECTED DISTANCES AND ANGLES FOR NbPdTe₅

Nb-2Te(5)	2.834(2)	Te(1)-Nb-2Te(2)	74.58(6)
Nb-2Te(2)	2.844(2)	Te(1)-Nb-2Te(5)	69.67(5)
Nb-2Te(3)	2.879(2)	Te(1)-Nb-2Te(3)	137.68(4)
Nb-Te(4)	2.883(3)	Te(1)-Nb-Te(4)	124.64(8)
Nb-Te(1)	2.947(3)	Te(2)-Nb-2Te(3)	69.01(5)
Nb-2Nb	3.728(2)	Te(2)-Nb-Te(2)	81.92(7)
Nb-2Pd	4.337(3)	Te(2)-Nb-2Te(5)	87.08(5)
Pd-2Te(4)	2.667(2)	Te(2)-Nb-2Te(4)	137.11(4)
Pd-2Te(1)	2.683(2)	Te(3)-Nb-Te(3)	80.70
Pd-Te(2)	2.704(2)	Te(3)-Nb-2Te(4)	74.42(5)
Pd-Te(3)	2.708(2)	Te(3)-Nb-2Te(5)	87.38(5)
Pd-2Pd	3.728(2)	Te(4)-Nb-2Te(5)	69.37(5)
Te(1)-2Te(5)	3.303(2)	Te(5)-Nb-2Te(5)	82.26(7)
Te(1)-2Te(2)	3.509(2)	Te(1)-Pd-Te(1)	88.01(7)
Te(1)-2Te(1)	3.728(2)	Te(1)-Pd-2Te(4)	91.63(4)
Te(1)-Te(2)	3.765(2)	Te(1)-Pd-2Te(2)	81.29(5)
Te(1)-Te(4)	3.836(2)	Te(1)-Pd-2Te(3)	100.82(6)
Te(1)-Te(3)	3.858(2)	Te(2)-Pd-Te(3)	177.02(7)
Te(2)-Te(3)	3.242(2)	Te(2)-Pd-2Te(4)	97.06(6)
Te(2)-2Te(5)	3.666(2)	Te(3)-Pd-2Te(4)	80.83(5)
Te(2)-2Te(2)	3.728(2)	Te(4)-Pd-Te(4)	88.68(7)
Te(3)-2Te(4)	3.485(2)		
Te(3)-2Te(3)	3.728(2)		
Te(4)-2Te(5)	3.254(2)		
Te(4)-Te(5)	3.718(2)		
Te(4)-2Te(4)	3.728(2)		
Te(5)-2Te(5)	3.728(2)		

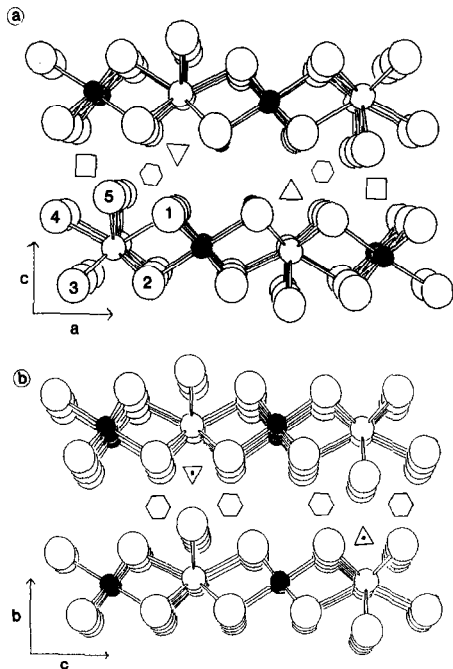


FIG. 1. View of NbPdTe_5 down the b axis (needle axis) showing the labeling scheme. Here and in Fig. 2a small filled circles are Pd atoms, small open circles are Nb atoms, and large open circles are Te atoms. \square , Octahedral vacancies; Δ , trigonal prismatic vacancies; and \circ , square pyramidal vacancies. (b) View of NbNiTe_5 down the a axis (needle axis). Here and in Fig. 2b small filled circles are Ni atoms, small open circles are Nb atoms, and large open circles are Te atoms. \circ , Square pyramidal vacancies; and Δ , tetrahedral vacancies.

even though the materials crystallize in different space groups: NbNiTe_5 , $Cmcm$; NbPdTe_5 , $Pnma$. In fact, the composition of the layers is almost identical. Table VI compares selected interatomic distances in NbPdTe_5 and NbNiTe_5 . Almost all intralayer distances are comparable.

The most significant difference between these structures is the way the layers order relative to one another. For NbNiTe_5 (Fig. 1b) the chains of Nb atoms in one layer are aligned with the chains of Nb atoms in another layer (in the b direction). The same is true of the Ni chains. In NbPdTe_5 (Fig. 1a) the layers have been shifted relative to one

TABLE VI
COMPARISON OF IMPORTANT INTERATOMIC
DISTANCES IN NbPdTe_5 AND NbNiTe_5

	NbNiTe_5	NbPdTe_5
Range of Nb-Te	2.808(3)–2.921(3)	2.834(2)–2.947(3)
Range of M-Te	2.557(3)–2.574(2)	2.667(2)–2.708(2)
Shortest Nb-Nb	3.656(5)	3.728(2)
Shortest M-M	3.656(5)	3.728(2)
Shortest Te-Te	3.196(4)	3.242(2)
Shortest interlayer Nb-M	4.200(4)	4.337(3)
Shortest interlayer Te-Te	3.789(3)	3.666(2)

another and now the chains of Nb atoms in one layer are aligned with chains of Pd atoms in another layer (in the c direction). This difference in the ordering of layers leads to different vacancies between layers. The vacancies in NbNiTe_5 are square pyramidal and tetrahedral while the vacancies in NbPdTe_5 are octahedral, square pyramidal, and trigonal prismatic. Figures 1a and 1b show the positions of the vacancies.

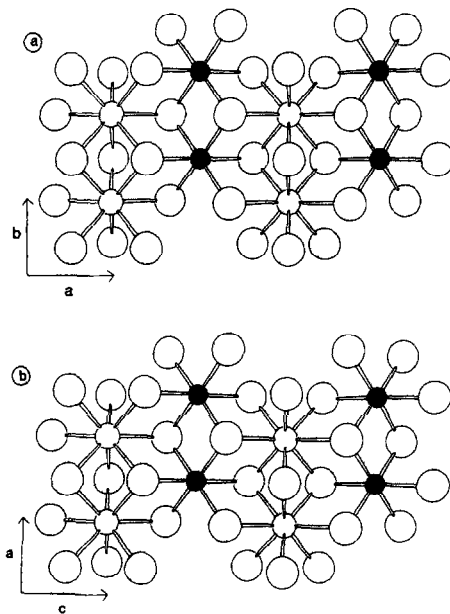


FIG. 2. (a) View of NbPdTe_5 down the a axis showing the coordination around the Nb and Pd atoms. (b) View of NbNiTe_5 down the b axis showing the coordination around the Nb and Ni atoms.

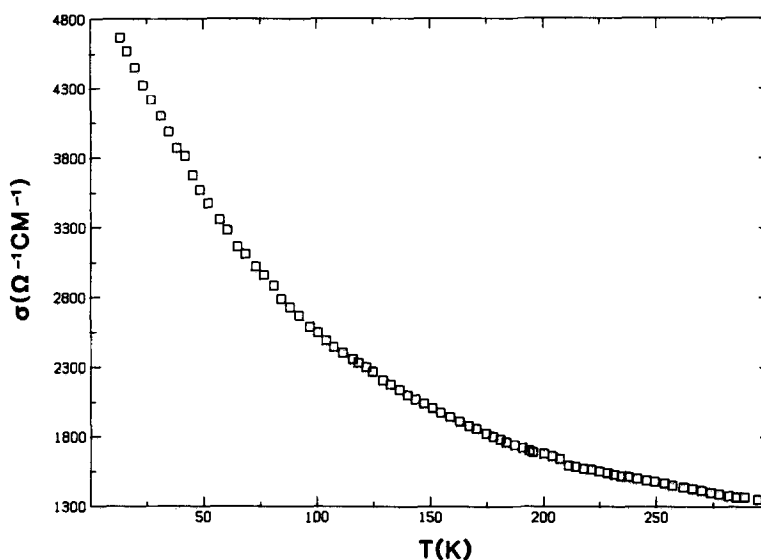


FIG. 3. Plot of conductivity vs temperature for NbPdTe₅.

While only octahedral and tetrahedral vacancies are present in binary layered chalcogenides, vacancies other than octahedral and tetrahedral are found in ternary chalcogenides (17, 18).

The Te-Te interactions in both of these compounds range from 3.18 to 3.8 Å. These distances are significantly longer than that of a full Te-Te bond (2.92 Å) (4), but much shorter than twice the ionic radius of Te (4.4 Å) (19). Thus, intermediate Te-Te interactions are present in both compounds. There are no short metal-metal interactions in these structures, as the shortest Nb-Nb, Ni-Ni, or Pd-Pd interaction is along the needle axis and is longer than 3.7 Å. This distance can be compared to the Nb-Nb distance of 3.029(2) Å found in NbCl₄ (20). The shortest Nb-M interactions in these compounds occur between layers at a distance greater than 4.2 Å.

Four-probe single-crystal conductivity measurements along the needle axis *b* show that NbPdTe₅ is metallic. A plot of the electrical conductivity over the temperature range 13–295 K is given in Fig. 3. A plot of the electrical conductivity of NbNiTe₅,

which was also measured along the needle axis, is given in Fig. 4.² There is a tremendous difference in the conductivity behavior of NbPdTe₅ and NbNiTe₅. NbNiTe₅ is a highly conductive metal ($\sigma_{10} > 5 \times 10^5 \Omega^{-1} \text{cm}^{-1}$) and NbPdTe₅ is a rather poor conductor ($\sigma_{10} \approx 4.7 \times 10^3 \Omega^{-1} \text{cm}^{-1}$).

Is the difference in the stacking of the layers or substitution of Pd for Ni the major reason for this conductivity difference? To attempt to answer this question we first note that for the isostructural binary compounds NiTe (21) and PdTe (22) and the isostructural binary compounds NiTe₂ (23) and PdTe₂ (24) the conductivity of the Pd compound is approximately equal to that of the corresponding Ni compound. Thus, the substitution of Pd for Ni has very little effect on the conductivity in the binary Pd and Ni tellurides. In the present system the metal-metal distances are sufficiently long to preclude any significant metal-metal overlap either between or within a layer.

² Conductivity data for NbNiTe₅ (Fig. 4) differ below 90 K from those reported previously (1); as it turns out those data were obtained on an instrument at the limit of its sensitivity.

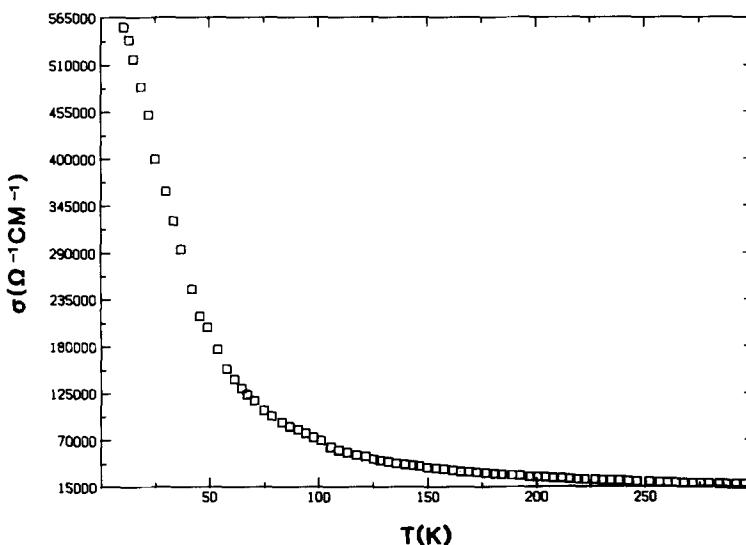


FIG. 4. Plot of conductivity vs temperature for NbNiTe₅.

The conductivity is measured along the needle axis (i.e., perpendicular to the plane of the paper of Figs. 1a and 1b). Thus, the conductivity is measured parallel to the chains of metal polyhedra and strictly within one layer. However, Te-Te orbital overlap must be important since these two compounds crystallize in different structural types even though the layers themselves are so similar.

Thus the cause of the difference in conductivity is not clear. A band structure calculation might be useful in this regard.

Acknowledgments

This research was supported by the U.S. National Science Foundation, Solid State Chemistry, Grant DMR-83-15554 and in part by NATO Research Grant 86-0438. This work made use of Central Facilities supported by the National Science Foundation through Northwestern University Materials Research Center, Grant DMR 85-20280. We are indebted to Prof. Carl Kannewurf for helpful discussions and for assistance with the conductivity measurements on NbNiTe₅.

References

1. E. W. LIIMATTA AND J. A. IBERS, *J. Solid State Chem.* **71**, 384 (1987).
2. E. W. LIIMATTA AND J. A. IBERS, *J. Solid State Chem.*, in press.
3. S. VAN SMAALEN, K. D. BRONSEMA, AND J. MAHY, *Acta Crystallogr. Sect. B* **42**, 43 (1986).
4. K. D. BRONSEMA, S. VAN SMAALEN, J. L. DE BOER, G. A. WIEGERS, F. JELLINEK, AND J. MAHY, *Acta Crystallogr. Sect. B* **43**, 305 (1987).
5. M. H. VAN MAAREN AND G. M. SCHAEFFER, *Phys. Lett. A* **24**, 645 (1967).
6. F. W. BOSWELL, A. PRODAN, AND J. K. BRANDON, *J. Phys. C*, **16**, 1067 (1983).
7. F. W. BOSWELL AND A. PRODAN, *Mater. Res. Bull.* **19**, 93 (1984).
8. J. BARSTAD, F. GRØNVOLD, E. RØST, AND E. VESTERSJØ, *Acta Chem. Scand.* **20**, 2865 (1966).
9. S. FURUSETH, K. SELTE, AND A. KJEKSHUS, *Acta Chem. Scand.* **19**, 257 (1965).
10. H. IPSE AND W. SCHUSTER, *J. Less-Common Met.* **125**, 183 (1986).
11. Program from Tracorn Northern, Madison, Wisconsin.
12. T. E. PHILLIPS, J. R. ANDERSON, C. J. SCHRAMM, AND B. M. HOFFMAN, *Rev. Sci. Instrum.* **50**, 263 (1979).
13. J. M. WATERS AND J. A. IBERS, *Inorg. Chem.* **16**, 3273 (1977).
14. J. A. IBERS AND W. C. HAMILTON (Eds.), "International Tables for X-ray Crystallography," Vol. IV, Tables 2.2A and 2.3.1, Kynoch Press, Birmingham (1974).
15. J. A. IBERS AND W. C. HAMILTON, *Acta Crystallogr.* **17**, 781 (1964).

16. G. M. SHELDRIK, in "Crystallographic Computing 3" (G. M. Sheldrick, C. Kruger, and R. Goddard, Eds.), pp. 175-189, Oxford Univ. Press, Oxford (1985).
17. P. J. SQUATTRITO, S. A. SUNSHINE, AND J. A. IBERS, *Solid State Ionics* **22**, 53 (1986).
18. S. A. SUNSHINE AND J. A. IBERS, *Inorg. Chem.* **24**, 3611 (1985).
19. R. D. SHANNON, *Acta Crystallogr. Sect. A* **32**, 751 (1976).
20. D. R. TAYLOR, J. C. CALABRESE, AND E. M. LARSEN, *Inorg. Chem.* **16**, 721 (1977).
21. S. FUJIME, M. MURAKAMI, AND E. HIRAHARA, *J. Phys. Soc. Japan* **16**(2), 183 (1961).
22. A. KJEKSHUS AND W. B. PEARSON, *Canad. J. Phys.* **43**, 438 (1965).
23. E. VANDENBEMPT, L. PAUWELS, AND K. DE CLIPPELEIR, *Bull. Soc. Chim. Belg.* **80**, 283 (1971).
24. A. LYONS, D. SCHLEICH, AND A. WOLD, *Mater. Res. Bull.* **11**(9), 1155 (1976).